ANTIOXIDANTS & REDOX SIGNALING
Volume 12, Number 7, 2010

DOI: 10.1089/ars.2009.2913

SECIS-Binding Protein 2 Promotes Cell Survival by Protecting Against Oxidative Stress

Laura V. Papp,[1] Jun Lu,[2] Emma Bolderson,[1] Didier Boucher,[1] Ravindra Singh,[3] Arne Holmgren,[2] and Kum Kum Khanna[1]

Abstract

Reactive oxygen species (ROS) are a primary cause of cellular damage that leads to cell death. In cells, protection from ROS-induced damage and maintenance of the redox balance is mediated to a large extent by selenoproteins, a distinct family of proteins that contain selenium in form of selenocysteine (Sec) within their active site. Incorporation of Sec requires the Sec-insertion sequence element (SECIS) in the 3′-untranslated region of selenoproteins mRNAs and the SECIS-binding protein 2 (SBP2). Previous studies have shown that SBP2 is required for the Sec-incorporation mechanism; however, additional roles of SBP2 in the cell have remained undefined. We herein show that depletion of SBP2 by using antisense oligonucleotides (ASOs) causes oxidative stress and induction of caspase- and cytochrome *c*-dependent apoptosis. Cells depleted of SBP2 have increased levels of ROS, which lead to cellular stress manifested as 8-oxo-7,8-dihydroguanine (8-oxo-dG) DNA lesions, stress granules, and lipid peroxidation. Small-molecule antioxidants *N*-acetylcysteine, glutathione, and α-tocopherol only marginally reduced ROS and were unable to rescue cells fully from apoptosis, indicating that apoptosis might be directly mediated by selenoproteins. Our results demonstrate that SBP2 is required for protection against ROS-induced cellular damage and cell survival. *Antioxid. Redox Signal.* 12, 797–808.

Introduction

Oxidative stress has been implicated in the initiation and progression of many human diseases, including cancer, neurodegenerative diseases, immune dysfunction, and aging (7, 36). Production of reactive oxygen species (ROS) that exceeds the antioxidant defense capacity of the cell causes various types of cellular injury including DNA damage, protein damage, and lipid peroxidation (36). Thus, levels of ROS modulate the physiologic state of the cell, and when oxidative-damaged biomolecules accumulate above a defined threshold, the cell undergoes apoptosis. Apoptosis represents a regulated form of cell death that requires the action of proteases and nucleases and takes place within an intact plasma membrane (38). At least two main pathways lead to apoptosis: an extrinsic (receptor dependent) and an intrinsic (mitochondrial) pathway. Both pathways involve activation of the family of cysteine proteases named caspases, which orchestrate dismantling of the cell for efficient removal by phagocytosis (17). In the intrinsic pathway, intracellular stress may promote signaling pathways or cause direct mitochondrial damage, leading to loss of mitochondrial membrane potential and release of proapoptotic molecules such as cytochrome *c* (Cyt c) from the mitochondrial intermembrane space into the cytosol (38, 48). Additional distinguishing features of apoptotic cell death include fragmentation of nuclear DNA, membrane blebbing, and cellular decomposition into apoptotic bodies, which are subsequently removed by phagocytosis (27).

To defend against the potentially deleterious effects of ROS, cells maintain an antioxidative capacity consisting of water- or lipid-soluble antioxidant compounds such as glutathione (GSH), ascorbate, α-tocopherol (α-Toc or vitamin E), as well as antioxidant enzyme systems that eliminate ROS through enzymatic reactions. Two of the main antioxidant enzyme systems in the cell contain the selenoproteins glutathione peroxidases (GPxs) and thioredoxin reductases (TrxRs) (31, 32). Members of the GPx family directly degrade hydrogen peroxide, organic hydroperoxides, and reduce oxidized phospholipids at the expense of GSH. TrxRs have a wide substrate range, including disulfide bonds in proteins and low-molecular-weight compounds (32). TrxRs, as part of the thioredoxin system, also serve important functions in intracellular redox regulation, signaling pathways, and apoptosis

[1]Signal Transduction Laboratory, Queensland Institute of Medical Research, Herston, Queensland, Australia.
[2]Division of Biochemistry, Department of Medical Biochemistry and Biophysics, Karolinska Institute, Stockholm, Sweden.
[3]Department of Biomedical Sciences, College of Veterinary Medicine, Iowa State University, Ames, Iowa.

(31). In addition to antioxidant protection and redox regulation, selenoproteins are involved in thyroid hormone metabolism (deiodinases 1, 2 and 3; DIO1, DIO2, and DIO3), selenocysteine (Sec) synthesis (selenophosphate synthetase 2; SPS2), transport and storage of selenium (selenoprotein P; Sel P), and protein folding in the endoplasmic reticulum (ER) (15-kDa selenoprotein, Sep15; selenoproteins N, M and S; Sel M, Sel N and Sel S) (32). Importantly, the enzymatic activity of selenoproteins depends on the presence of Sec within the active site. Because Sec is encoded by UGA (28), which usually serves as translation termination, its decoding as Sec requires several unique, evolutionarily conserved structures and protein factors. The major cis-acting determinant for Sec incorporation is the Sec-insertion sequence (SECIS) element, a stem-loop RNA structure located within the 3′-untranslated region of all eukaryotic selenoprotein mRNAs (8, 9). Additional factors include the Sec $tRNA^{[Ser]Sec}$ (28), the SECIS-binding protein 2 (SBP2) (13, 14), the Sec-specific elongation factor eEFSec (20, 46), the ribosomal protein L30 (11), the 43-kDa RNA binding protein (SECp43), and Sec synthase (47).

SBP2, the most extensively studied Sec-incorporation factor, contains an RNA-binding domain that directly interacts with the SECIS element, which is required for the incorporation of Sec at defined UGA codons. This has now been demonstrated *in vitro*, in cell-culture models, and *in vivo* (15, 19, 30, 33). Several mutations in the SBP2 gene (*SECISBP2*) that cause a dramatic reduction in the amounts of functional SBP2 have been described in patients with clinical abnormalities in thyroid hormone metabolism (18, 19). Although the thyroid phenotype was directly attributed to reduction in the DIO2 enzyme activity, GPx1 activity and Sel P levels were also decreased in the patients, indicating a global reduction in selenoprotein synthesis and confirming SBP2 as epistatic to this process. Mouse studies have demonstrated that selenoproteins are essential for life, as the complete deletion of Sec $tRNA^{[Ser]Sec}$ is embryonic lethal (10). Based on the fact that partial depletion of SBP2 results in a global decrease in selenoproteins, it can be predicted that the complete loss of SBP2 would have a lethal outcome.

Antisense inhibition of gene expression is a technology widely used to evaluate gene function *in vitro* and *in vivo* (39). The second-generation antisense oligonucleotides (ASOs) consist of ~20 nucleotides complementary to the target pre-mRNA or mRNA and contain nucleotide and backbone modifications that increase their stability and affinity toward their target. These ASOs do not recruit RNase H to degrade the complex, and thus their antisense effect is only due to steric hindrance of splicing or translation.

We previously used short-hairpin RNAs (shRNA) to deplete SBP2 in cells and obtained an approximate 50% reduction in SBP2 protein levels, which led to a modest reduction in downstream effects such as selenoprotein synthesis and cell viability in unchallenged cells (33). In a more recent study, we used ASO technology to alter splicing of SBP2 (34) and observed that knockdown at the protein level was almost complete. We therefore used this technology to study the effects of an almost complete depletion of SBP2 in cells, by using three different ASOs targeted against SBP2 pre-mRNA or mRNA. All three ASOs were extremely efficient at depleting SBP2 protein levels, which led to rapid induction of apoptosis in several cancer cell lines. Moreover, depletion of SBP2 caused substantial oxidative stress, leading to DNA damage, stress-granule formation, lipid peroxidation, and cell-cycle arrest. Our data suggest that SBP2 is a crucial molecule within the cellular antioxidant defense and is required for cell survival.

Materials and Methods

Cell culture, reagents, and treatments

Human cervical carcinoma HeLa cells, human osteosarcoma U2OS cells, and normal skin fibroblast (NFF) cells were cultured in RPMI 1640 medium supplemented with 10% heat-inactivated fetal bovine serum (Invitrogen, Carlsbad, CA), 100 units/ml penicillin, and 100 μg/ml streptomycin. U2OS cells stably expressing SBP2 were selected and grown in media containing 100 μg/ml zeocin (Invitrogen). HeLa cells overexpressing BCL-2 were kindly provided by Nigel Waterhouse (Mater Medical Research Institute, Brisbane, Australia).

H_2O_2 (200 μM; Sigma, St. Louis, MO) in phosphate-buffered saline (PBS) was added to cells for 20 min to induce oxidative stress. Caspase inhibitor z-VAD-fmk (Biosource International, Camarillo, CA) (100 μM) was added at 6 h after ASO transfection and left until cell harvest for the time indicated. All antioxidants were added to the culture media 24 h before transfection. α-Toc (Sigma) was diluted in ethanol and added to culture media at 100 μM. Glutathione reduced ethyl ester (GSSE) (Sigma) and *N*-acetylcysteine (NAC) (Sigma) were diluted in water and added to culture media at concentration of 1 m*M* and 5 m*M*, respectively.

Antibodies used in this study include mouse anti-7,8-dihydro-8-oxoguanine (8-oxodG) (Chemicon International); mouse anti-PARP1 (Zymed); rabbit anti-caspase-3 (Biosource); mouse anti-β-actin (Sigma); goat anti-TIA-1 (Santa Cruz, SC1751); mouse ATM 2C1 (GeneTex); mouse ATM Ser 1981 (Cell Signalling); mouse γ-H2Ax (Millipore); rabbit SBP2 in house (33); goat Gpx4 (Everest Biotech); rabbit TrxR1 (Upstate); goat TrxR2 (Santa Cruz); goat Grx1 and goat thioredoxin (IMCO Ltd., Stockholm, Sweden).

ROS and lipid peroxidation measurement

ROS were measured by using the 2′,7′-dichlorodihydrofluorescein diacetate (H_2DCFDA) probe (Fluka). The H_2DCFDA probe was dissolved in anhydrous dimethyl formamide (DMF) (Sigma), and cells were labeled with 2 μM H_2DCFDA diluted in PBS for 30 min at 37°C and 5% CO_2 followed by 30-min recovery in RPMI media. BODIPY581/591 C_{11} was dissolved in anhydrous DMF, and cells were labeled with 1 μM BODIPY581/591 C_{11} diluted in PBS for 1 h at 37°C and 5% CO_2.

Antisense oligonucleotide sequences and plasmid construction

ASOs were synthesized by Dharmacon, Inc. The sequences are control ASO: mG*mA*mU*mC*mG*mA*mU*mC*mG*mA*mU*mC*mG*mA*mU*mC*mG*mA*mU*mC*mG*mA; In2E3a ASO: mC*mU*mG*mC*mC*mU*mA*mA*mG*mU*mA*mA*mA*mA*mA*mG*mU*mG*mU*mA*mA*mA*mC; In4E5 ASO: mC*mC*mA*mU*mC*mU*mG*mU*mA*mA*mU*mU*mA*mC*mA*mA*mA*mA*mU*mU*mA*mA*mA; E3a3b ASO: mG*mA*mG*mU*mA*mA*mA*mC*mA*mU*mU*mC*mU*mG*mU*mG*mU*mG*mG*mA*mG*mU*mC. The letter m represents an *O*-methyl modification at the second position of a sugar residue, and an asterisk represents a phosphorothioate

modification of the backbone. ASOs were transfected into cells by using Lipofectamine 2000 (Invitrogen) at a final concentration of 100 n*M*.

Generation of stable SBP2-expressing cells

To make stable SBP2-expressing cells, we used the ViraPower T-REx Lentiviral Expression System (Invitrogen) according to the manufacturer's instruction. In brief, SBP2 cDNA was subcloned into the lentiviral expression vector Lenti4TO/V5. 293T-FT packaging cells were transfected with SBP2Lenti4TO/V5 vector or Lenti4TO/V5 empty vector with Lipofectamine 2000 transfection reagent (Invitrogen). Media containing virus were collected at 48 h after transfection and used immediately for infection of target U2OS cells. U2OS cells were selected with zeocin (Invitrogen), starting 48 h after viral transduction for a duration of ~7–10 days.

Annexin V assay and cytochemical staining

HeLa cells were transfected with ASOs. At the time indicated, all cells (including floating ones) were collected, washed once in PBS, and resuspended in 100 μl 1x annexin V binding buffer (10 m*M* HEPES, 140 m*M* NaCl, and 2.5 m*M* $CaCl_2$, pH 7.4). Then 5 μl of anti-Annexin V antibody (Molecular Probes) and 1 μl propidium iodide (PI) (1 mg/ml) were added to cells and incubated for 20 min. After incubation, 400 μl of 1x annexin V binding buffer was added, and cells were analyzed by fluorescence-activated cell sorting (FACS). The cell populations staining positive for annexin V and negative for PI and staining positive for annexin V and positive for PI were regarded as apoptotic.

Apoptosis was alternatively evaluated with fluorescence microscopy after cytochemical staining with 4',6-diamidino-2-phenylindole (DAPI). Cells grown on coverslips and treated as indicated were washed with PBS, fixed in 4% paraformaldehyde, and permeabilized with 0.1% Triton X-100 for 10 min at room temperature. The fixed cells were stained with DAPI for 5 min, washed, and then examined with fluorescence microscopy (340-nm excitation and 510-nm barrier filter) by using an IM1000Leica DMIRB microscope equipped with a 40x objective. Apoptotic cells were identified by the presence of highly condensed or fragmented nuclei. At least five fields and a minimum of 200 cells per field was scored per coverslip. Nuclei with fragmented DNA were calculated as a percentage of the total number of nuclei. Statistical analysis was performed by using Prism 5.

Immunofluorescence microscopy and immunoblotting

Immunofluorescence microscopy and immunoblotting were performed as described previously (34). 8-Oxodg staining was performed as described previously (44).

Cell-cycle analysis

DNA synthesis was assayed by using the Click-iT EdU Cell Proliferation Assays (Invitrogen) as per manufacturer's instructions. In brief, at 16 h after ASO transfection, cells were incubated with 5-bromo-2-deoxyuridine (BrdU) for 1 h to detect newly synthesized DNA and with 7-amino-actinomycin D (7-AAD) to detect total genomic DNA. Cells were analyzed with flow cytometry by using a FACS Scan sorter (Becton Dickinson), and the number of cells in S phase quantified by using ModFit. For analysis of cells in G_1 and G_2 phases of the cell cycle, cells were harvested by scraping, washed in PBS, and fixed in 70% ice-cold methanol overnight at −20°C. Cells were subsequently washed twice in PBS, and treated cells with ribonuclease (100 μg/ml) for 30 min at 37°C. PI (50 μg/ml) was added, the cells were analyzed with flow cytometry, and the number of cells in G_1 and G_2 were quantified by using ModFit. To measure G_1 arrest, nocodazole (0.2 μg/ml) was added to cells at 8 h after transfection, and incubation was continued for 14 h. Cells were harvested and processed for FACS sorting, as described earlier.

Results

ASO-mediated depletion of SBP2 leads to rapid induction of apoptosis

Three different ASOs were designed to deplete SBP2 in cells: In2E3a and In4E5, complementary to the intron 2-exon 3a and intron 4-exon 5 boundaries, respectively, and E3a3b, complementary to the exon 3a-exon 3b boundary. In contrast to the partial reduction of SBP2 achieved by using shRNA (33), all three SBP2 ASOs, but not control ASO, led to a strong reduction of SBP2 protein levels in HeLa cells by 24 h after transfection (Fig. 1A). We hence took advantage of the efficient ASO-mediated knockdown system to study the function of SBP2 in cells.

The first observation after ASO transfection was a large amount of cell death that appeared specific to SBP2-ASO–transfected cells, because very little death was observed in the control ASO-transfected cells. To determine the type of cell death, we performed annexin V labeling, a widely used assay for differentiation of apoptosis from necrosis, and analyzed the samples by FACS. Quantitation of annexin V–positive/PI-negative and annexin V–positive/PI-positive cells revealed that ~30% of cells depleted of SBP2 were apoptotic at 16 h after transfection and ~60% at 24 h after transfection (Fig. 1B), indicating that ASO-mediated depletion of SBP2 led to induction of apoptosis. Apoptosis also was assayed by using cytochemical staining for nuclear fragmentation, yielding a similar proportion of apoptotic cells (Fig. 1C). Both methods were used throughout the study.

Further to substantiate these results, we investigated additional key events of apoptosis such as caspase 3 (Casp 3) activation by proteolytic cleavage of its procaspase form, cleavage of poly-ADP ribose polymerase-1 (PARP1) and Cyt c release from the mitochondria into the cytosol. As shown in Fig. 1D, PARP1 cleavage, procasp 3 cleavage, and Cyt c release were clearly evident in SBP2-depleted cells, and occurred to a similar extent in cells undergoing ultraviolet irradiation type C–induced apoptosis (data not shown).

To test whether SBP2 depletion–induced apoptosis is caspase dependent or independent, we co-treated ASO-transfected cells with the general caspase inhibitor z-VAD-fmk, and quantified DAPI-stained cells for nuclear DNA fragmentation. As shown in Fig. 1E, z-VAD-fmk treatment completely blocked cell death, suggesting that SBP2 depletion–induced apoptosis requires caspase activation. Because caspase activation can be induced through the intrinsic or the extrinsic apoptotic pathways, we next investigated which of the two pathways is predominantly responsible for inducing SBP2-mediated apoptosis. Initiation of the intrinsic apoptotic program requires Cyt c release from the mitochondria into the

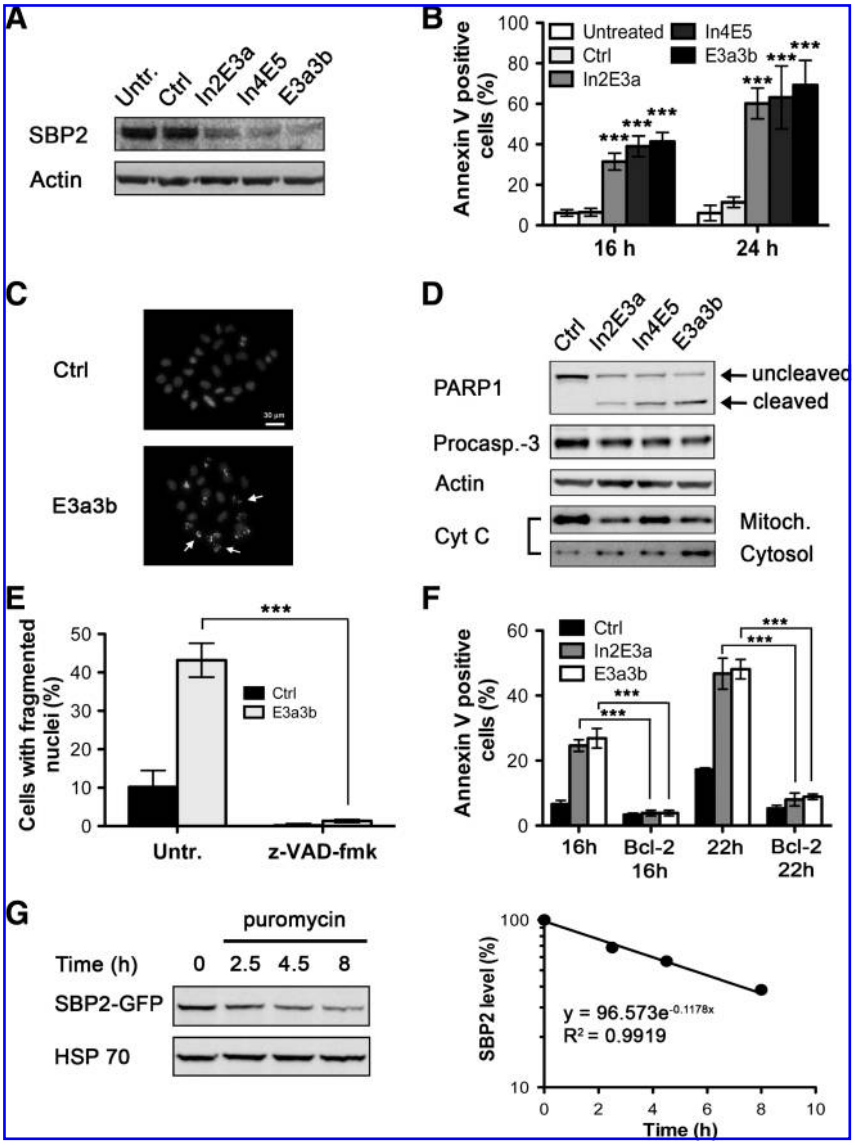

FIG. 1. SBP2 depletion leads to caspase- and mitochondria-dependent induction of apoptosis. HeLa cells were transfected with control (ctrl) ASO and three different ASOs against SBP2: In2E3a, In4E5, and E3a3b. (**A**) SBP2 protein levels were determined with Western blotting at 20 h after transfection. Actin was used as a loading control. (**B**) FACS analysis of annexin V fluorescent labeling was performed 16 h and 24 h after ASO transfection. Graph shows the average percentage of annexin V–positive cells from four independent experiments (±SD; two-way ANOVA; $***p < 0.001$). (**C**) DAPI staining at 16 h after transfection with ctrl and E3a3b ASOs. *Arrows*, Apoptotic cells with fragmented nuclei. (**D**) Western blotting of PARP1 cleavage, procaspase 3 activation, and Cyt c release from the mitochondria into the cytosol, 20 h after ASO transfection. (**E**) Caspase inhibition with z-VAD-fmk prevents SBP2 depletion–induced apoptosis. Quantitation of the percentage of untreated or z-VAD-fmk–treated HeLa cells with fragmented nuclei 16 h after ctrl or E3a3b ASO transfection as measured with DAPI staining. Percentages were calculated from 1,000 cells in two independent experiments (±SD; *t* test; $***p < 0.0001$). (**F**) FACS analysis of annexin V fluorescent labeling in HeLa cells or HeLa cells stably overexpressing Bcl-2 at 16 h and 22 h after ctrl In2E3a and E3a3b ASO transfection. Graph shows the average percentage of annexin V–positive cells from three independent experiments (±SD; *t* test; $***p < 0.001$). (**G**) HeLa cells were transfected with SBP2-GFP plasmid, and 24 h later, puromycin (200 μg/ml) was added to block translation. Samples were collected at the times indicated and probed with anti-SBP2 antibodies. Hsp 70 was used as loading control. Bands were quantified with densitometry, and the protein half-life was calculated with logarithmic regression.

cytosol, which is inhibited by Bcl-2 overexpression (26, 48). By using the previously characterized Bcl-2–overexpressing HeLa cells (41), we confirmed that SBP2 depletion–induced apoptosis requires mitochondrial signaling activation (Cyt c release), as shown by an almost complete inhibition of apoptosis by Bcl-2 overexpression (Fig. 1F). Together, these results indicate that SBP2 depletion–induced apoptosis is triggered through the intrinsic apoptotic pathway.

The rapid onset of apoptosis observed after ASO transfection prompted us to investigate the half-life of SBP2. HeLa cells transfected with an SBP2 green fluorescent protein-tagged expression plasmid (SBP2-GFP) were treated with

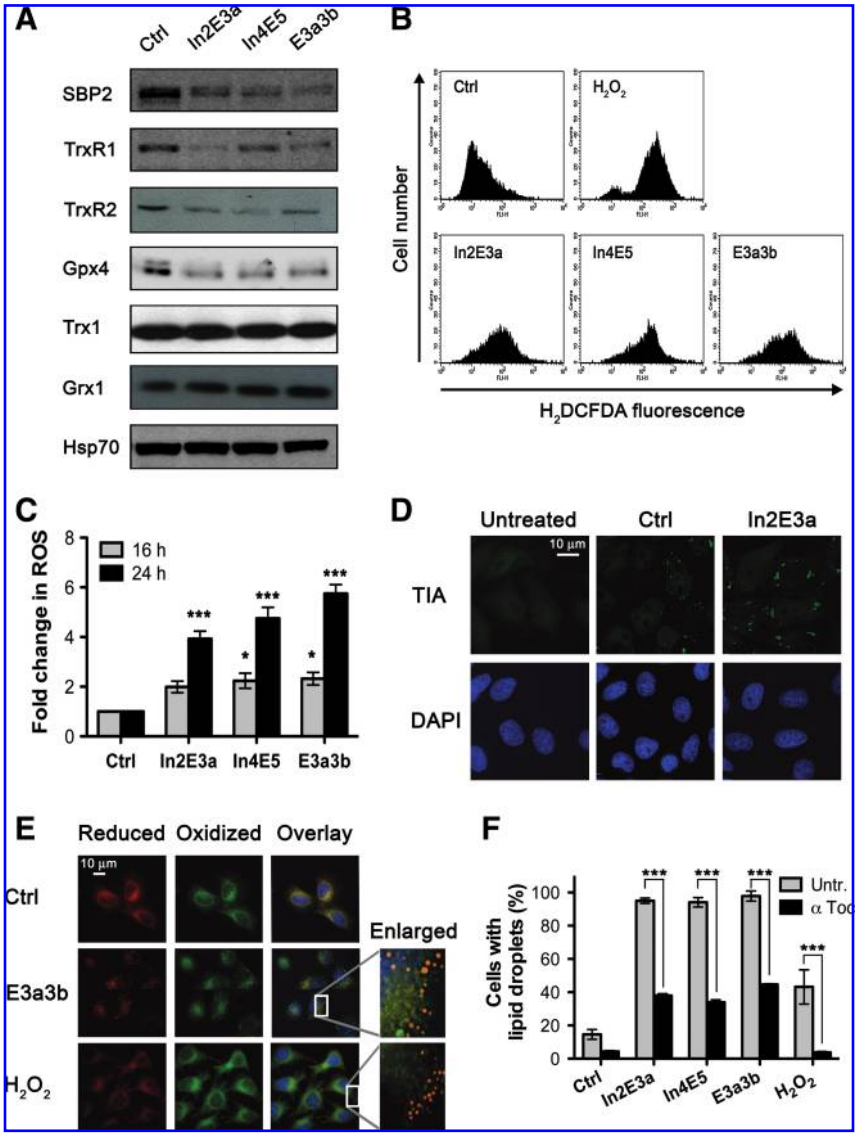

FIG. 2. SBP2 depletion leads to decreased levels of selenoproteins, high levels of ROS, and oxidative stress. (**A**) Western blot analysis of SBP2, TrxR1, TrxR2, GPx4, Trx1, and Grx1 protein levels in control, In2E3a, In4E5, and E3a3b ASO-transfected HeLa cells. Hsp70 was used as a loading control. (**B**) HeLa cells transfected with control, In2E3a, In4E5, and E3a3b ASOs or treated with H_2O_2 for 20 min were stained with the soluble redox-sensitive probe H_2DCFDA for 30 min at 24 h after transfection and analyzed with FACS. Graphs show a shift in the probe fluorescence peak, indicating accumulation of ROS. (**C**) Average relative ROS levels measured with H_2DCFDA fluorescence at 16 h and 24 h after ASO transfection (±SD; two-way ANOVA; $^*p < 0.05$; $^{***}p < 0.001$). (**D**) Stress granule (SG) formation after control and In2E3a transfection of HeLa cells. SGs were observed with immunofluorescence staining of the TIA-1 SG marker (green) at 16 h after transfection. Nuclei (blue) were stained with DAPI. (**E**) Lipid peroxidation was measured with the BODIPY581/591 C_{11} probe in cells at 18 h after transfection with control and E3a3b ASO, or after treatment with 200 μM H_2O_2 for 20 min. The reduced form of the probe (red) was observed at 546 nm, and the oxidized form (green), at 488 nm. Nuclei (blue) were stained with DAPI. All images were acquired and deconvolved with a Deltavision Personal DV microscope. Enlarged pictures correspond to a zooming of the white rectangle of the overlay images for E3a3b and H_2O_2. (**F**) Quantitation lipid droplets (LDs), 20 h after transfection with indicated ASOs or treatment with 200 μM H_2O_2, in the absence or presence of α-Toc. A minimum of 300 cells was counted at 546 nm per coverslip. The graph represents the average number of cells with LDs from two independent experiments (±SD; *t* test; $^{***}p < 0.001$). (For interpretation of the references to color in this figure legend, the reader is referred to the web version of this article at www.liebertonline.com/ars).

puromycin to block translation, and SBP2-GFP protein levels were measured with immunoblotting at several time points after puromycin addition. By using logarithmic regression, we determined that in HeLa cells, SBP2 has a half-life of 5.6 h (Fig. 1G). Thus, the timing of apoptosis induction on ASO transfection is in keeping with the declining SBP2 protein levels. It should be noted that on entering the cell, ASOs do not require processing and are therefore able to act on their substrate pre-mRNA or mRNA immediately. SBP2 depletion–induced cell death also was evident in other cancer cell lines including C33A, MSTO, U2OS, LNCap, MCF7, as well as in primary NFFs; however, the timing of apoptosis onset after

ASO transfection was delayed in NFF cells compared with cancer cells, likely reflecting the difference in their metabolic rate, and also in LNCap and MCF7 cells because of the existence of inherent mutations in genes involved in the regulation of apoptosis (data not shown).

SBP2 depletion leads to high levels of ROS, stress granule formation, and lipid peroxidation

The known SBP2 function in the cell is to control the synthesis of selenoproteins, which protect against oxidative stress and damage to proteins, lipids, and nucleic acids. Next, we verified by Western blotting and Se^{75} labeling that selenoprotein levels were indeed reduced as a result of ASO-mediated SBP2 depletion. A clear reduction in TrxR1, TrxR2, and GPx4 protein levels was observed in SBP2-depleted cells (Fig. 2A). Moreover, levels of the antioxidant protein thioredoxin 1 (Trx1) remained unchanged, whereas the levels of glutaredoxin 1 (Grx1) were increased by ~30%, 40%, and 70% in the three SBP2 ASO–depleted lanes, respectively, as measured with densitometry (Fig. 2A). A global decrease in selenoprotein synthesis after SBP2 ASO transfection was also observed by Se^{75} labeling, as reported previously (33).

Next, we set to determine whether SBP2-mediated apoptosis could be attributed to increased intracellular oxidative stress, as a result of decreased selenoprotein expression, by measuring the levels of ROS with FACS by using the redox-sensitive probe H_2DCFDA. On oxidation, H_2DCFDA becomes fluorescent, which is detected as a shift in fluorescence emission peak. As shown in Fig. 2B, the H_2DCFDA fluorescence peak is indeed shifted in SBP2 ASO–transfected and H_2O_2-treated cells as compared with control ASO cells, indicating the presence of ROS in the cells. Already at 16 h after ASO transfection, the H_2DCFDA fluorescence was about twofold higher in SBP2-depleted than in control HeLa cells, which further increased to about fivefold by 24 h (Fig. 2C). Because cells were already undergoing apoptosis at these time points, and apoptosis *per se* can cause an increase in intracellular ROS (38), we measured H_2DCFDA fluorescence in SBP2-depleted cells treated with z-VAD-fmk, which completely inhibited apoptosis (Fig. 1E). Interestingly, z-VAD-fmk treatment did not inhibit ROS formation in SBP2-ASO transfected cells (data not shown), confirming that ROS generation is a result of SBP2 depletion.

One of the many responses of a eukaryotic cell to oxidative stress is to shut down protein synthesis to conserve energy for the repair of stress-induced damage. This process involves the formation of cytoplasmic foci known as stress granules (SGs), which consist of eukaryotic initiation factor eIF2/eIF5-deficient preinitiation complexes and their associated mRNA transcripts, small ribosomal subunits, translation factors, and RNA-binding proteins. SG assembly requires the two RNA-binding proteins, TIA-1 and TIAR (2). As a measure of oxidative stress, we next investigated SG formation in SBP2-depleted cells, by immunofluorescence staining for the SG marker TIA-1. Indeed, ~80% of SBP2-ASO–transfected cells displayed TIA-1 localization to SGs, as compared with about 30% of control ASO-transfected cells (Fig. 2D). Although transfection *per se* seemed to cause a small induction of SGs, the SG induction in SBP2-depleted cells was considerably higher.

Lipid peroxidation is another well-known downstream effect of oxidative stress. It was recently reported that deletion of GPx4 leads to lipid peroxidation–induced apoptosis, which was completely rescued by the antioxidant α-Toc (42). Prompted by these findings and our results showing significantly decreased GPx4 protein levels in SBP2-depleted cells, we analyzed the extent of lipid peroxidation in ASO-transfected cells with the redox-sensitive, lipid-specific dye, BODIPY581/591 C_{11}. H_2O_2 was used as a comparative oxidative stress–inducing agent. The most striking observation after BODIPY581/591 C_{11} staining was that cells depleted of SBP2 displayed a substantial increase in lipid body/lipid droplet (LD) formation, as shown in Fig. 2E. LDs were also formed in response to H_2O_2 treatment; however, in the H_2O_2-treated cells, the LDs were fewer, smaller, and their accumulation was concentrated to the cell periphery, whereas in SBP2-depleted cells, LDs were more numerous, larger, and distributed throughout the cytoplasm (Fig. 2E and enlargement). LDs showed both red fluorescence, representing the reduced form of BODIPY581/591 C_{11}, and green fluorescence, representing the oxidized form. Notably, the green fluorescence was stronger toward the periphery of the droplets (Fig. 2E, enlargement), indicating the presence of oxidized lipids. LDs are present in most eukaryotic cells, where they form an integral part of intracellular lipid storage and transport (21). LD formation can be triggered by oxidative stress, as also shown in a recent study (24). Supplementation with α-Toc before and during ASO transfection attenuated LD formation by more than half in SBP2-depleted cells, and completely prevented it in H_2O_2-treated cells (Fig. 2F). Collectively, these results suggest that SBP2 depletion causes decreased selenoprotein synthesis, high levels of ROS leading to intracellular oxidative stress.

Depletion of SBP2 causes DNA damage and cell-cycle arrest

It is well established that oxidative stress causes DNA damage, which in turn can lead to apoptosis (38). 8-Oxo-7,8-dihydroguanine (8-oxo-dG) is regarded as the most ubiqui-

FIG. 3. SBP2 depletion causes DNA damage and cell-cycle arrest. (**A**) Immunofluorescence staining of 8-oxo-dG in HeLa cells, 16 h after transfection with control and In2E3a ASOs, or treated with 200 μM H_2O_2 as positive control. DNA was stained with DAPI. Images were acquired and deconvolved with Deltavision Personnal DV microscope. (**B**) Western blots of HeLa cell extracts 16 h after transfection with control, In2E3, In4E5, and E3a3b ASOs showing phosphorylation of ATM at Ser 1981 (P-ATM(S1981), total ATM levels, and phosphorylation of H2AX (γ-H2AX). Actin was used as loading control. (**C**) Immunofluorescence staining of γ-H2AX in control and E3a3b ASO-transfected HeLa cells. (**D**) Quantitation of cells positive for γ-H2AX foci in control, In2E3a, In4E5, and E3a3b ASO-transfected HeLa cells (±SD; one-way ANOVA; $^{**}p < 0.01$). A minimum of 300 cells was counted in each of two independent experiments. (**E**) SBP2 depletion–induced γ-H2AX foci formation in In2E3a-transfected HeLa and HeLa Bcl-2 cells. (**F**) FACS analysis of BrdU labeling 18 h after ASO transfection of HeLa cells. Each graph shows the level of BrdU (y-axis, FL1-H) relative to DNA content stained by 7-AAD (x-axis, FL4-A). (**G**) Cell-cycle analysis of untreated or nocodazole-treated HeLa cells at 16 h after transfection with control, In4E5, and E3a3b ASO, as measured by FACS after PI staining. (For interpretation of the references to color in this figure legend, the reader is referred to the web version of this article at www.liebertonline.com/ars).

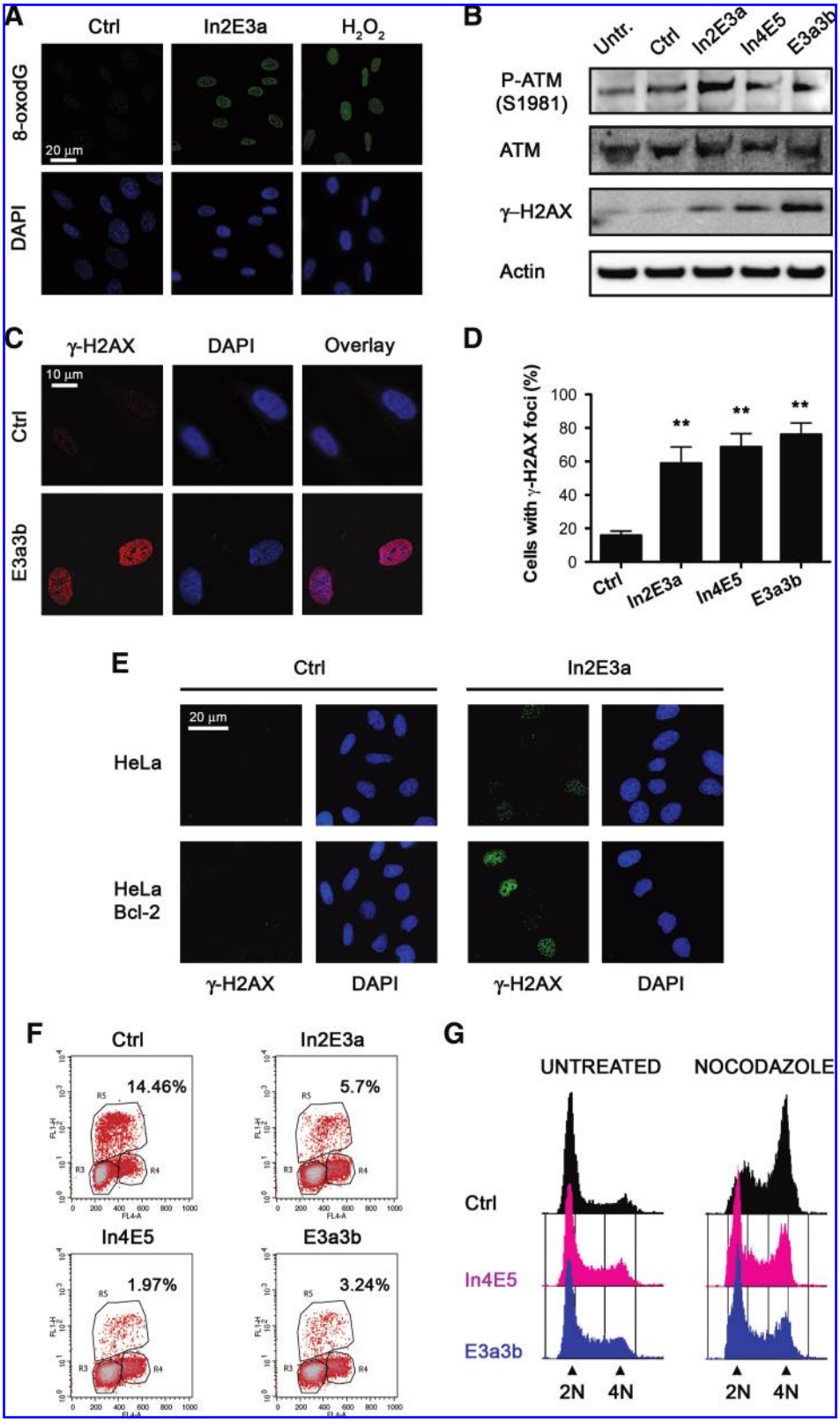

tous oxidative DNA lesion, and it often serves as a marker for cellular oxidative stress (1). Immunostaining for 8-oxo-dG revealed that SBP2-depleted cells have increased oxidative DNA damage at 18 h after transfection, which was comparable to H_2O_2-induced DNA damage (Fig. 3A). The early intracellular DNA-damage response (DDR) involves autophosphorylation of Ataxia Telangiectasia Mutated (ATM) on residue serine (Ser) 1981, and phosphorylation of the histone variant H2AX (phosphorylated form is named γ-H2AX) (5, 37). After DNA double-strand breaks (DSBs) induction,

γH2AX is associated with the formation of nuclear foci containing factors that are essential for DNA repair, replication, and cell-cycle regulation, which is critical for protecting the genome from spontaneous DSBs (12, 35). As shown by Western blotting in Fig. 3B, ATM-Ser1981 and H2AX phosphorylation were both induced in SBP2-depleted cells. Moreover, γ-H2AX localization to damage-induced foci was detected in ~60–80% of SBP2-depleted cells (Fig. 3C and D). Interestingly, In2E3a-transfected Bcl-2 overexpressing HeLa cells that failed to undergo apoptosis showed stronger-intensity γ-H2AX staining than In2E3a-transfected HeLa cells, representing a continuous accumulation of DNA damage due to lack of apoptosis (Fig. 3E).

Cell-cycle checkpoint activation and cell-cycle arrest are hallmarks of DDR-pathway activation (23). Because lack of checkpoint activation would compromise the DNA-repair capacity and lead to increased propensity to undergo apoptosis, we investigated the activation of checkpoint response in SBP2-depleted cells by measuring the percentage of cells incorporating BrdU, which is indicative of actively replicating cells in S phase. Cells depleted of SBP2 had a significant reduction of percentage of cells in S phase, which could be due to the activation of the G_1/S checkpoint, which stops the progression of cells with DNA damage from G_1 into S phase (Fig. 3F). We further verified G_1 arrest by treatment with nocodazole, a microtubule poison, which causes the accumulation of actively cycling cells in G_2, allowing the quantitation of cells already arrested in G_1 (22). As expected, control ASO-transfected HeLa cells showed a clear accumulation of cells in G_2 and reduction of cells in G_1 in response to nocodazole treatment (from ~70% to ~3%); however, SBP2-depleted cells showed only a minor reduction of cells in G_1 (from ~55% to ~35%) (apoptotic cells were gated out in the analysis, hence the absence of the sub-G_1 peaks) (Fig. 3G). This suggests that SBP2 depletion–induced DNA damage causes G_1 arrest and normal checkpoint activation. However, it is possible that an imbalance in the induction of DNA damage *versus* cellular DNA-repair capacity, caused by excessive accumulation of damage in SBP2-depleted cells, overwhelms the DNA-repair pathway, which might contribute to induction of apoptosis in these cells. This possibility is interesting from many aspects, in particular, the fact that so far, selenoproteins have not been directly implicated in DNA repair, and thus this issue warrants further investigation that was not pursued in this study.

Antioxidants do not prevent SBP2 depletion–induced apoptosis

Our results so far have demonstrated that efficient depletion of SBP2 in cells leads to protein, lipid, and DNA damage, and ultimately to apoptosis. At least two mechanistic explanations for the SBP2-induced apoptosis are possible: in one scenario, apoptosis could be due to the lack of particular selenoproteins with direct antiapoptotic function; the second explanation could be an overall increase in ROS as a result of a global decrease in selenoprotein-mediated antioxidant defense. We thus hypothesized that if apoptosis were due to ROS, supplementation with antioxidants should prevent both ROS induction and apoptosis. To test this, cells were grown in the presence of the antioxidants α-Toc, which prevents lipid peroxidation; reduced glutathione in the stabilized form, glutathione ethyl ester (GSSE); *N*-acetylcysteine (NAC); a general antioxidant that promotes induction of GSH; or a mixture of all antioxidants (Mix) for 24 h before transfection. As shown in Fig. 4A, α-Toc, GSSE, or NAC individually did not reduce the number of apoptotic cells; the Mix of antioxidants had a modest yet significant effect. Conversely, we found that all antioxidants were able to reduce ROS levels significantly in SBP2-depleted cells, with the best effects (more than 50% reduction compared with unsupplemented cells) seen with the Mix supplementation (Fig. 4B). It should also be noted that the concentration of antioxidants was titrated, and the use of higher concentrations led to an increase in ROS (data not shown).

Finally, we generated a full-length SBP2 construct resistant to the In2E3a and In4E5 ASOs and expressed it stably in U2OS cells by using lentiviral transduction. Notably, the overexpression of SBP2 was only slightly higher than the endogenous SBP2 levels (Fig. 4C). In2E3a ASO treatment led to a significant decrease in SBP2 protein levels in the parental cell line, but only to a slight decrease in the ASO-resistant SBP2-expressing cells, representing the knockdown of the endogenous SBP2 (Fig. 4D). Apoptosis was reduced to control levels in the ASO-resistant SBP2-overexpressing cells, whereas the parental cells showed normal signs of apoptosis (Fig. 4E). These results confirm that apoptosis is indeed triggered by SBP2 depletion, as it could be prevented by overexpression of the ASO-resistant SBP2.

Discussion

It is widely known that ROS modulate the physiological state of the cell and influence apoptosis. Exogenous prooxidant agents such as H_2O_2 or menadione can induce apoptosis in a variety of cell types because of excessive ROS production and intracellular damage (29). Conversely, redox homeostasis and normal cell growth are kept in balance by antioxidant enzyme systems, including selenoproteins, which in turn depend on the presence of SBP2 (32). Here, we demonstrate that SBP2 is required for cell growth and viability (Fig. 5). We show that ASO-mediated depletion of SBP2 in cells leads to oxidative stress–induced damage to several subcellular compartments, including the nucleus (DNA damage), the cytosol (LD formation), and the ER (SG formation). These effects can most likely be attributed to the lack of selenoprotein function in these compartments. The cumulative damage ultimately leads to induction of the classic type of mitochondria- and caspase 3–dependent apoptosis.

Squires *et al*. (43) recently showed that cells partially depleted of SBP2 display a reduction in telomere length (43), which could be caused by oxidative DNA damage or defective DNA replication. Our data showing that depletion of SBP2 indeed leads to accumulation of 8-oxodG oxidative DNA lesions is consistent with their findings and provides the evidence that the cause of telomere shortening in the absence of SBP2 is due to oxidative damage. The study did not find any differences in the growth rates or viability of SBP2-depleted cells, which is explained by the partial SBP2 knockdown.

Several selenoproteins have been implicated in protection against apoptosis. GPx4 is a crucial sensor and transducer of oxidative stress signals into 12/15 lipoxygenase-dependent and apoptosis-initiation factor (AIF)-mediated apoptosis (42).

GPx4 depletion causes severe lipid peroxidation that is completely preventable by α-Toc supplementation (42). In contrast, α-Toc was unable to rescue the SBP2 depletion–induced apoptosis, thus ruling out lipid peroxidation or loss of GPx4 as the sole cause of apoptosis. Furthermore, pathways responsible for induction of apoptosis due to deficiency of GPx4 or SBP2 are different in terms of the requirement for casp 3. Sel S (also called SEPS1), an ER-resident selenoprotein, has been shown to have a specific protective effect against ER stress–induced apoptosis when overexpressed, whereas its suppression sensitized cells to ER stress–induced cell death (25). Our data showing SG formation in SBP2-depleted cells clearly indicates that ER stress was present, thus suggesting the possibility that the resulting Sel S depletion might be a

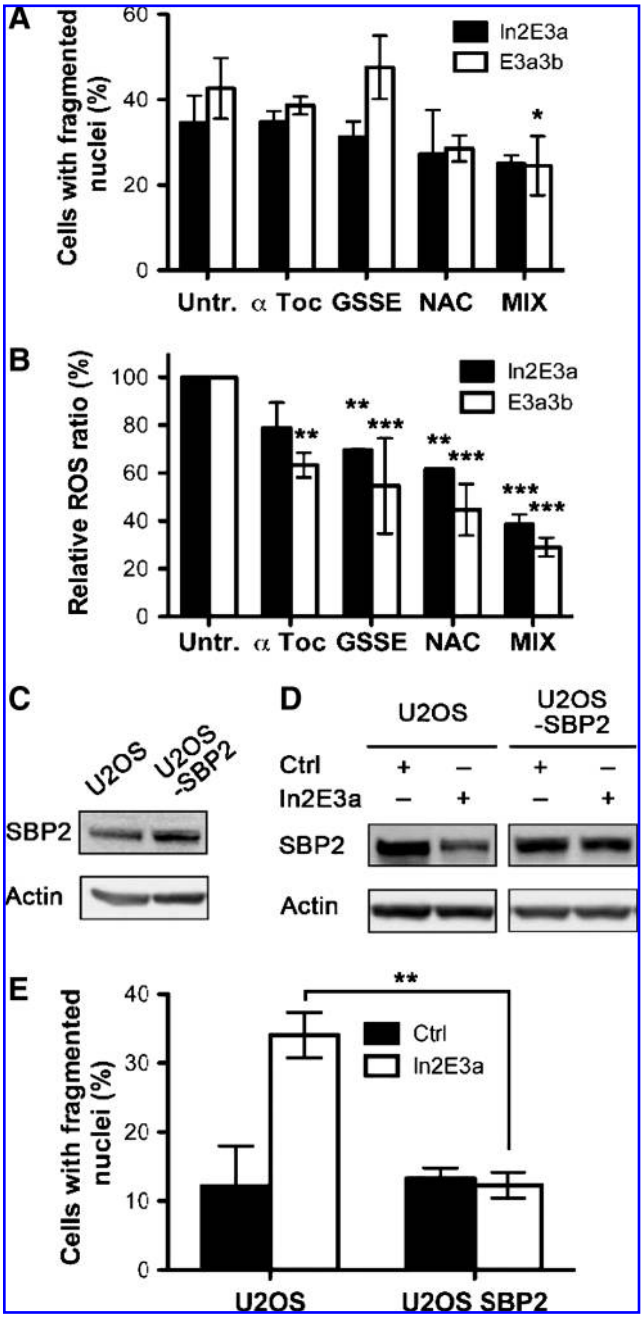

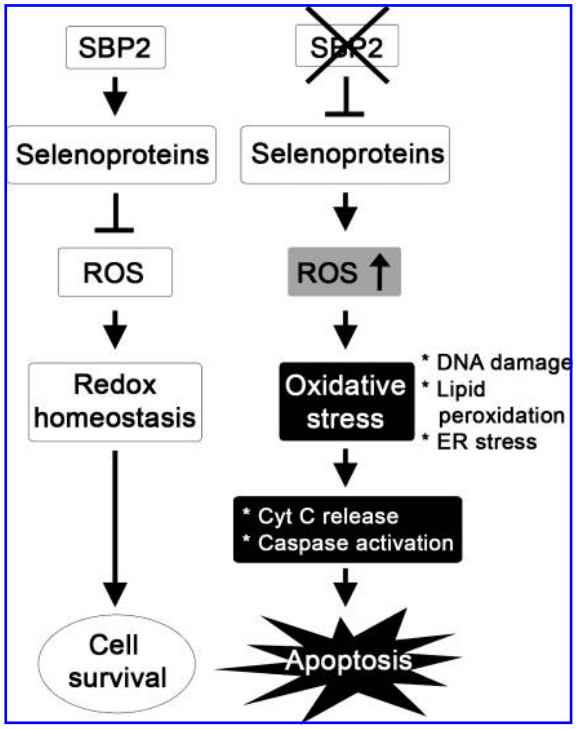

FIG. 5. Model of SBP2 depletion–induced apoptosis. SBP2 maintains adequate levels of selenoproteins, which prevent increases in ROS levels and promote intracellular redox homeostasis. In case of SBP2 depletion below a certain threshold, selenoprotein synthesis is diminished, leading to high levels of ROS, which in turn cause intracellular oxidative stress. Excess oxidative damage manifested in the form of DNA damage, lipid peroxidation, and ER stress leads to induction apoptosis initiated by cytochrome *c* release from the mitochondria, which subsequently triggers the activation of caspase 3 and the execution of apoptosis.

FIG. 4. Antioxidants do not prevent SBP2 depletion–induced apoptosis. (**A**) Quantitation of the percentage of HeLa cells with fragmented nuclei 16 h after ASO transfection in unsupplemented cells (untr.) or in cells supplemented with α-Toc, GSSE, NAC, and combined antioxidants (Mix). Nuclei were stained with DAPI and scored by using an IM1000Leica DMIRB microscope. Percentages were calculated from 1,000 cells per experiment (±SD; two-way ANOVA; $^{*}p < 0.05$). (**B**) Relative ROS levels measured with H_2DCFDA fluorescence at 16 h after ASO transfection. Values for each antioxidant were normalized to the corresponding ASO in the unsupplemented sample. The graph shows the average relative H_2DCFDA fluorescence from triplicate samples in one representative experiment (±SD; two-way ANOVA; $^{**}p < 0.01$; $^{***}p < 0.001$). (**C**) Western blot shows the expression of SBP2 in U2OS cells and in U2OS cells stably expressing SBP2 (U2OS-SBP2), generated by lentiviral transduction. (**D**) Western blot shows depletion of SBP2 in In2E3a-transfected U2OS cells but not in the ASO-resistant U2OS-SBP2 cells. Actin shows protein loading. (**E**) Quantitation of nuclear fragmentation as measured by DAPI staining in U2OS and stable U2OS-SBP2 cells, 16 h after control and In2E3a ASO transfection. Percentages were calculated from 1,000 cells observed per experiment in two independent experiments (±SD; *t* test; $^{**}p < 0.01$).

contributing factor in SBP2 depletion–induced apoptosis. Sel H overexpression was shown to have a protective effect against UVB-induced apoptosis by directly reducing the superoxide anion formation (6). Furthermore, a Sec-compromised TrxR1 enzyme has been shown to promote cell death in cancer cell lines owing to gain-of-function effects (3). Cells transfected directly with purified TrxR1 protein lacking the penultimate Sec amino acid undergo rapid induction of caspase-mediated cell death. This also correlated with an increase in intracellular oxidative stress; however, cell death was prevented by antioxidants. Chemical inhibition of TrxR1 with its specific inhibitor auranofin also triggered apoptosis through the Bax/Bak-dependent pathway because of mitochondria-selective oxidative stress (16). In this study, we found a large reduction in total TrxR1 protein levels in SBP2-depleted cells, and, given the crucial role of TrxR1 in many processes closely linked to cell viability (4), it is highly likely that loss of TrxR1 is one of the main contributing factors to apoptosis induction in SBP2-depleted cells.

Small molecule antioxidants such as NAC or α-Toc have been widely shown to suppress apoptosis directly by acting as ROS scavengers. In selenium deficiency–induced necrosis or GPx4-induced apoptosis, α-Toc or other vitamin E derivatives were able to rescue cell death independent of selenoprotein activity (40, 42). In this study, despite being able to reduce ROS levels partially, antioxidants were not able to prevent apoptosis, thus suggesting that the combined loss of selenoprotein redox capacity causes severe oxidative stress, and, in some subcellular compartments such as mitochondria, the redox balance change may play a direct role in SBP2 depletion–induced apoptosis.

An interesting comparison of the effect of global selenoprotein depletion is the conditional Sec $tRNA^{Sec}$ (*Trsp*) gene-deletion model. Conditional deletion of *Trsp* in macrophages led to elevated levels of ROS and increased intracellular oxidative stress, however, with no adverse effects on cell viability (45). Interestingly, a concurrent NF-E2–related factor 2 (Nrf2)–mediated transcriptional induction of non-selenoprotein antioxidant enzymes was found to provide a compensatory effect on the loss of protective selenoprotein activity. When the *Trsp*/*Nrf2* double-knockout system was generated, this compensatory induction was lost, and cell death by both apoptotic and necrotic features was apparent in both cultured macrophages and liver (45). In view of these findings, it is somewhat intriguing that depletion of SBP2 alone, which ultimately should have the same effect on selenoprotein production as *Trsp* gene deletion, has such a dramatic impact on cell viability.

Similar to the *Trsp* deletion, we also found a transcriptional induction of several antioxidant genes, including glutathione *S*-transferases (GSTs), and heme oxygenase 1 (HO-1) in response to SBP2 depletion (unpublished observations), and we are currently investigating this further. Nevertheless, this induction does not appear sufficient to prevent the detrimental accumulation of intracellular oxidative damage and apoptosis. In the context of the model of global selenoprotein depletion, it is also not excluded that SBP2 may have an additional function in the cell, independent of selenoprotein expression, yet related to maintenance of cell viability. It would be interesting to investigate the levels of oxidative stress and DNA damage in patients with known mutations in *SECISBP2* (18, 19) and thus compromised selenoprotein capacity and to determine whether these patients would benefit from a long-term supplementation with antioxidants to prevent the detrimental accumulation of ROS-induced cellular damage.

Acknowledgments

This work was supported by the National Health and Medical Research Council program grant (K.K.K), and by the Swedish Cancer Society (961), the Swedish Research Council Medicine (13x-3529), the K.A. Wallenberg Foundation, and the Karolinska Institutet (A.H.).

Disclosure Statement

No competing financial interests exist.

References

1. Altieri F, Grillo C, Maceroni M, and Chichiarelli S. DNA damage and repair: from molecular mechanisms to health implications. *Antioxid Redox Signal* 10: 891–937, 2008.
2. Anderson P and Kedersha N. Stressful initiations. *J Cell Sci* 115: 3227–3234, 2002.
3. Anestal K and Arner ES. Rapid induction of cell death by selenium-compromised thioredoxin reductase 1 but not by the fully active enzyme containing selenocysteine. *J Biol Chem* 278: 15966–15972, 2003.
4. Arner ES and Holmgren A. Physiological functions of thioredoxin and thioredoxin reductase. *Eur J Biochem* 267: 6102–6109, 2000.
5. Bakkenist CJ and Kastan MB. DNA damage activates ATM through intermolecular autophosphorylation and dimer dissociation. *Nature* 421: 499–506, 2003.
6. Ben Jilani KE, Panee J, He Q, Berry MJ, and Li PA. Overexpression of selenoprotein H reduces Ht22 neuronal cell death after UVB irradiation by preventing superoxide formation. *Int J Biol Sci* 3: 198–204, 2007.
7. Benz CC and Yau C. Ageing, oxidative stress and cancer: paradigms in parallax. *Nat Rev Cancer* 8: 875–879, 2008.
8. Berry MJ, Banu L, Chen YY, Mandel SJ, Kieffer JD, Harney JW, and Larsen PR. Recognition of UGA as a selenocysteine codon in type I deiodinase requires sequences in the 3′ untranslated region. *Nature* 353: 273–276, 1991.
9. Berry MJ, Banu L, Harney JW, and Larsen PR. Functional characterization of the eukaryotic SECIS elements which direct selenocysteine insertion at UGA codons. *EMBO J* 12: 3315–3322, 1993.
10. Bosl MR, Takaku K, Oshima M, Nishimura S, Taketo MM. Early embryonic lethality caused by targeted disruption of the mouse selenocysteine tRNA gene (Trsp). *Proc Natl Acad Sci U S A* 94: 5531–5534, 1997.
11. Chavatte L, Brown BA, and Driscoll DM. Ribosomal protein L30 is a component of the UGA-selenocysteine recoding machinery in eukaryotes. *Nat Struct Mol Biol* 12: 408–416, 2005.
12. Chen HT, Bhandoola A, Difilippantonio MJ, Zhu J, Brown MJ, Tai X, Rogakou EP, Brotz TM, Bonner WM, Ried T, and Nussenzweig A. Response to RAG-mediated VDJ cleavage by NBS1 and gamma-H2AX. *Science* 290: 1962–1965, 2000.
13. Copeland PR and Driscoll DM. Purification, redox sensitivity, and RNA binding properties of SECIS-binding protein 2: a protein involved in selenoprotein biosynthesis. *J Biol Chem* 274: 25447–25454, 1999.

14. Copeland PR, Fletcher JE, Carlson BA, Hatfield DL, and Driscoll DM. A novel RNA binding protein, SBP2, is required for the translation of mammalian selenoprotein mRNAs. *EMBO J* 19: 306–314, 2000.
15. Copeland PR, Stepanik VA, and Driscoll DM. Insight into mammalian selenocysteine insertion: domain structure and ribosome binding properties of Sec insertion sequence binding protein 2. *Mol Cell Biol* 21: 1491–1498, 2001.
16. Cox AG, Brown KK, Arner ES, and Hampton MB. The thioredoxin reductase inhibitor auranofin triggers apoptosis through a Bax/Bak-dependent process that involves peroxiredoxin 3 oxidation. *Biochem Pharmacol* 76: 1097–1109, 2008.
17. Czerski L and Nunez G. Apoptosome formation and caspase activation: is it different in the heart? *J Mol Cell Cardiol* 37: 643–652, 2004.
18. Di Cosmo C, McLellan N, Liao XH, Khanna KK, Weiss RE, Papp L, and Refetoff S. Clinical and molecular characterization of a novel selenocysteine insertion sequence-binding protein 2 (SBP2) gene mutation (R128X). *J Clin Endocrinol Metab* 94: 4003–4009, 2009.
19. Dumitrescu AM, Liao XH, Abdullah MS, Lado-Abeal J, Majed FA, Moeller LC, Boran G, Schomburg L, Weiss RE, and Refetoff S. Mutations in SECISBP2 result in abnormal thyroid hormone metabolism. *Nat Genet* 37: 1247–1252, 2005.
20. Fagegaltier D, Hubert N, Yamada K, Mizutani T, Carbon P, and Krol A. Characterization of mSelB, a novel mammalian elongation factor for selenoprotein translation. *EMBO J* 19: 4796–4805, 2000.
21. Goodman JM. The gregarious lipid droplet. *J Biol Chem* 283: 28005–28009, 2008.
22. Khanna KK, Beamish H, Yan J, Hobson K, Williams R, Dunn I, and Lavin MF. Nature of G1/S cell cycle checkpoint defect in ataxia-telangiectasia. *Oncogene* 11: 609–618, 1995.
23. Khanna KK, Lavin MF, Jackson SP, and Mulhern TD. ATM, a central controller of cellular responses to DNA damage. *Cell Death Differ* 8: 1052–1065, 2001.
24. Khatchadourian A and Maysinger D. Lipid droplets: their role in nanoparticle-induced oxidative stress. *Mol Pharm* 6: 1125–1137, 2009.
25. Kim KH, Gao Y, Walder K, Collier GR, Skelton J, and Kissebah AH. SEPS1 protects RAW264.7 cells from pharmacological ER stress agent-induced apoptosis. *Biochem Biophys Res Commun* 354: 127–132, 2007.
26. Kluck RM, Bossy-Wetzel E, Green DR, and Newmeyer DD. The release of cytochrome c from mitochondria: a primary site for Bcl-2 regulation of apoptosis. *Science* 275: 1132–1136, 1997.
27. Kroemer G, Dallaporta B, and Resche-Rigon M. The mitochondrial death/life regulator in apoptosis and necrosis. *Annu Rev Physiol* 60: 619–642, 1998.
28. Lee BJ, Worland PJ, Davis JN, Stadtman TC, and Hatfield DL. Identification of a selenocystenyl-tRNA(Ser) in mammalian cells that recognizes the nonsense codon, UGA. *J Biol Chem* 264: 9724–9727, 1989.
29. Lennon SV, Martin SJ, and Cotter TG. Dose-dependent induction of apoptosis in human tumour cell lines by widely diverging stimuli. *Cell Prolif* 24: 203–214, 1991.
30. Low SC, Grundner-Culemann E, Harney JW, and Berry MJ. SECIS-SBP2 interactions dictate selenocysteine incorporation efficiency and selenoprotein hierarchy. *EMBO J* 19: 6882–6890, 2000.
31. Lu J and Holmgren A. Selenoproteins. *J Biol Chem* 284: 723–727, 2009.
32. Papp LV, Lu J, Holmgren A, and Khanna KK. From selenium to selenoproteins: synthesis, identity, and their role in human health. *Antioxid Redox Signal* 9: 775–806, 2007.
33. Papp LV, Lu J, Striebel F, Kennedy D, Holmgren A, and Khanna KK. The redox state of SECIS binding protein 2 controls its localization and selenocysteine incorporation function. *Mol Cell Biol* 26: 4895–4910, 2006.
34. Papp LV, Wang J, Kennedy D, Boucher D, Zhang Y, Gladyshev VN, Singh RN, and Khanna KK. Functional characterization of alternatively spliced human SECISBP2 transcript variants. *Nucleic Acids Res* 36: 7192–7206, 2008.
35. Petersen S, Casellas R, Reina-San-Martin B, Chen HT, Difilippantonio MJ, Wilson PC, Hanitsch L, Celeste A, Muramatsu M, Pilch DR, Redon C, Ried T, Bonner WM, Honjo T, Nussenzweig MC, and Nussenzweig A. AID is required to initiate Nbs1/gamma-H2AX focus formation and mutations at sites of class switching. *Nature* 414: 660–665, 2001.
36. Potashkin JA and Meredith GE. The role of oxidative stress in the dysregulation of gene expression and protein metabolism in neurodegenerative disease. *Antioxid Redox Signal* 8: 144–151, 2006.
37. Rogakou EP, Pilch DR, Orr AH, Ivanova VS, and Bonner WM. DNA double-stranded breaks induce histone H2AX phosphorylation on serine 139. *J Biol Chem* 273: 5858–5868, 1998.
38. Ryter SW, Kim HP, Hoetzel A, Park JW, Nakahira K, Wang X, and Choi AM. Mechanisms of cell death in oxidative stress. *Antioxid Redox Signal* 9: 49–89, 2007.
39. Sahu NK, Shilakari G, Nayak A, and Kohli DV. Antisense technology: a selective tool for gene expression regulation and gene targeting. *Curr Pharm Biotechnol* 8: 291–304, 2007.
40. Saito Y, Yoshida Y, Akazawa T, Takahashi K, and Niki E. Cell death caused by selenium deficiency and protective effect of antioxidants. *J Biol Chem* 278: 39428–39434, 2003.
41. Sedelies KA, Ciccone A, Clarke CJ, Oliaro J, Sutton VR, Scott FL, Silke J, Susanto O, Green DR, Johnstone RW, Bird PI, Trapani JA, and Waterhouse NJ. Blocking granule-mediated death by primary human NK cells requires both protection of mitochondria and inhibition of caspase activity. *Cell Death Differ* 15: 708–717, 2008.
42. Seiler A, Schneider M, Forster H, Roth S, Wirth EK, Culmsee C, Plesnila N, Kremmer E, Radmark O, Wurst W, Bornkamm GW, Schweizer U, and Conrad M. Glutathione peroxidase 4 senses and translates oxidative stress into 12/15-lipoxygenase dependent- and AIF-mediated cell death. *Cell Metab* 8: 237–248, 2008.
43. Squires JE, Davy P, Berry MJ, and Allsopp R. Attenuated expression of SECIS binding protein 2 causes loss of telomeric reserve without affecting telomerase. *Exp Gerontol* 44: 619–623, 2009.
44. Suraweera A, Becherel OJ, Chen P, Rundle N, Woods R, Nakamura J, Gatei M, Criscuolo C, Filla A, Chessa L, Fusser M, Epe B, Gueven N, and Lavin MF. Senataxin, defective in ataxia oculomotor apraxia type 2, is involved in the defense against oxidative DNA damage. *J Cell Biol* 177: 969–979, 2007.
45. Suzuki T, Kelly VP, Motohashi H, Nakajima O, Takahashi S, Nishimura S, and Yamamoto M. Deletion of the selenocysteine tRNA gene in macrophages and liver results in compensatory gene induction of cytoprotective enzymes by Nrf2. *J Biol Chem* 283: 2021–2030, 2008.
46. Tujebajeva RM, Copeland PR, Xu XM, Carlson BA, Harney JW, Driscoll DM, Hatfield DL, and Berry MJ. Decoding

apparatus for eukaryotic selenocysteine insertion. *EMBO Rep* 1: 158–163, 2000.
47. Xu XM, Carlson BA, Mix H, Zhang Y, Saira K, Glass RS, Berry MJ, Gladyshev VN, and Hatfield DL. Biosynthesis of selenocysteine on its tRNA in eukaryotes. *PLoS Biol* 5: e4, 2007.
48. Yang J, Liu X, Bhalla K, Kim CN, Ibrado AM, Cai J, Peng TI, Jones DP, and Wang X. Prevention of apoptosis by Bcl-2: release of cytochrome c from mitochondria blocked. *Science* 275: 1129–1132, 1997.

Address correspondence to:
Laura V. Papp or Kum Kum Khanna
Cancer and Cell Biology Division
The Queensland Institute of Medical Research
300 Herston Road
Herston, QLD 4006
Australia

E-mail: kumkum.khanna@qimr.edu.au

Date of first submission to ARS Central, September 22, 2009; date of acceptance, October 3, 2009.

Abbreviations Used

ASO = antisense oligonucleotide
BrdU = 5-bromo-2-deoxyuridine
Cyt c = cytochrome *c*
DAPI = 4′,6-diamidino-2-phenylindole
DDR = DNA-damage response
DSBs = DNA double-strand breaks
GPxs = glutathione peroxidases
GSH = glutathione
GSSE = glutathione reduced ethyl ester
H_2DCFDA = 2′,7′-dichlorodihydrofluorescein diacetate
LD = lipid droplet
NAC = *N*-acetylcysteine
NFF = normal skin fibroblast
8-oxo-dG = 8-oxo-7,8-dihydroguanine
PARP1 = poly-ADP ribose polymerase-1
ROS = reactive oxygen species
SBP2 = SECIS-binding protein 2
Sec = selenocysteine
SECIS = Sec insertion sequence element
SGs = stress granules
α-Toc = α-tocopherol
TrxR = thioredoxin reductase

This article has been cited by:

1. Bryan A. Haines, Darcy A. Davis, Artem Zykovich, Botao Peng, Rammohan Rao, Sean D. Mooney, Kunlin Jin, David A. Greenberg. 2012. Comparative protein interactomics of neuroglobin and myoglobin. *Journal of Neurochemistry* **123**:1, 192-198. [CrossRef]
2. Lutz Schomburg. 2011. Selenium, selenoproteins and the thyroid gland: interactions in health and disease. *Nature Reviews Endocrinology* . [CrossRef]
3. Erik Schoenmakers, Maura Agostini, Catherine Mitchell, Nadia Schoenmakers, Laura Papp, Odelia Rajanayagam, Raja Padidela, Lourdes Ceron-Gutierrez, Rainer Doffinger, Claudia Prevosto, Jian'an Luan, Sergio Montano, Jun Lu, Mireille Castanet, Nick Clemons, Matthijs Groeneveld, Perrine Castets, Mahsa Karbaschi, Sri Aitken, Adrian Dixon, Jane Williams, Irene Campi, Margaret Blount, Hannah Burton, Francesco Muntoni, Dominic O'Donovan, Andrew Dean, Anne Warren, Charlotte Brierley, David Baguley, Pascale Guicheney, Rebecca Fitzgerald, Alasdair Coles, Hill Gaston, Pamela Todd, Arne Holmgren, Kum Kum Khanna, Marcus Cooke, Robert Semple, David Halsall, Nicholas Wareham, John Schwabe, Lucia Grasso, Paolo Beck-Peccoz, Arthur Ogunko, Mehul Dattani, Mark Gurnell, Krishna Chatterjee. 2010. Mutations in the selenocysteine insertion sequence–binding protein 2 gene lead to a multisystem selenoprotein deficiency disorder in humans. *Journal of Clinical Investigation* **120**:12, 4220-4235. [CrossRef]
4. Laura V. Papp , Arne Holmgren , Kum Kum Khanna . 2010. Selenium and Selenoproteins in Health and Disease. *Antioxidants & Redox Signaling* **12**:7, 793-795. [Abstract] [Full Text HTML] [Full Text PDF] [Full Text PDF with Links]